Simulation of Seismic Processes with High-Order Grid-Characteristic Methods

Vasily I. Golubev[1] ![ORCID], *Alexey V. Shevchenko*[1,2] ![ORCID]

This paper considers simulation of the seismic wave propagation in geological media with different rheological properties. The present work aims to construct a numerical scheme to model porous fluid-saturated medium, for the description of which the Dorovsky model was selected. We employed the grid-characteristic method, which includes choosing the appropriate operator splitting method for a 3D problem, deriving the transformation to the Riemann invariants analytically, and explicitly setting boundary and contact conditions. We simulated two scenarios. Firstly, we compared the wavefields generated by a point-source in the acoustic, linear elastic, and porous fluid-saturated approximations, noting the similarities in the longitudinal wave and differences in other wave types. Secondly, we simulated a part of the marine seismic survey process, including a source in the water layer, governed by the acoustic equations, a water-saturated layer described by the Dorovsky equations, and an explicit contact between these layers. To utilize the modern HPC multi-core and multi-processor systems, the hybrid MPI-OpenMP parallel algorithms were used.

Keywords: Dorovsky model, grid-characteristic method, contact conditions.

Introduction

The task of an accurate modelling of wave processes in deformable media is important in multiple different applications, such as non-destructive testing of composite materials, medical ultrasound imaging, seismic survey process, earthquake simulation, etc. If simple models prove to be insufficient, more complex and accurate ones are employed. It should be noted, that since analytical solutions are not available for most valuable mechanical problems, computer simulations are required.

Let us concentrate on the seismic wave propagation problem. The simplest model is the linear acoustic model [1, 10]. Despite its derivation for fluids, it has gained significant popularity, being a reasonably good choice for simulating only longitudinal waves in geological media. However, other types of waves (transverse waves, complex surface waves) often have to be taken into account, thus requiring more sophisticated models like the isotropic linear elastic model [1]. In other cases, more sophisticated properties need to be considered, for example, anisotropy. Another example of a medium with a complex internal structure is a porous fluid-saturated medium. One of its distinctive physical properties is the existence of the second longitudinal wave with a smaller velocity. Several mathematical models are used to describe it, the most popular one being the Biot model [3]. However, other models like the Dorovsky model [4, 11] are available as well. In our work we choose the Dorovsky model because it is governed by a hyperbolic system of PDEs and it only has three elastic parameters that uniquely define (or are defined by) the three velocities of wave propagation.

Since solving larger equations requires more computational resources, researchers attempt to use simpler models of the medium whenever possible. One option to do that is to combine several models in one simulation, which allows us to conduct highly accurate modelling and save

---

[1]Moscow Institute of Physics and Technology, Dolgoprudny, Russian Federation
[2]Ishlinsky Institute for Problems in Mechanics RAS, Moscow, Russian Federation

significant resources at the same time. Usually, each model is set on a separate grid; therefore, special contact conditions between those grids are required. These conditions have to be both physically and mathematically correct to ensure convergence towards the correct solution. Generally, such conditions do not depend upon the chosen numerical method; some examples can be found in the papers [6–8, 10].

Different numerical methods can be used to solve the governing equations. Most popular ones are the finite-difference and finite-element methods, but others can be used, too. In this work we use the grid-characteristic method, which is described in more details in the papers [5, 6, 8].

This paper has the following structure. Firstly, we describe the physical and mathematical models used in this study. Then we present the developed numerical method, including handling internal and boundary points and implementation of contact conditions. Finally, we show the results of several computer simulations.

1. Mathematical Models

Different models can be used for describing the process of seismic wave propagation in geological media. Here we only consider those which can take into account the wave fronts; they are usually represented in the form of systems of partial differential equations with necessary initial and boundary conditions.

1.1. Acoustic Equations

One of the basic models is the linear acoustic model. The equations are as follows [1, 10]:

$$\begin{cases} \rho \vec{v}_t & = -\nabla p + \vec{F}, \\ p_t & = -c^2 \rho \, \nabla \cdot \vec{v}. \end{cases} \tag{1}$$

Here, $p = p(x, y, z, t)$ is the acoustic pressure, $\vec{v} = \vec{v}(x, y, z, t)$ is the particle velocity (the derivative of the local displacement vector with respect to time). Force vector $\vec{F}(x, y, z, t)$ denotes the right-hand side, the applied external volumetric force. The known parameters (generally, space-dependent) are density ρ [kg/m^3] and wave speed c [m/s] ($c = \sqrt{K/\rho}$, where K is the bulk modulus).

Zero initial conditions are used, since unknowns p and $\vec{v}$ are relative to the steady state. One boundary condition is required; for instance, given pressure $P(x, y, z, t)\big|_{x,y,z \in \partial E}$. Here the computational domain is denoted as E and its boundary – as ∂E. Boundary condition $P \equiv 0$ sets the free surface, which is commonly used on top boundary.

Acoustic equations (1) accurately describe low-amplitude pressure waves (propagating with the speed c) in fluids.

1.2. Equations of Linear Elasticity

The system of PDEs for the linear elastic model is presented below [1, 5]:

$$\begin{cases} \rho \vec{v}_t = (\nabla \cdot \mathbf{T})^\intercal + \vec{F}, \\ \mathbf{T}_t = \lambda (\nabla \cdot \vec{v}) \mathbf{I} + \mu (\nabla \otimes \vec{v} + (\nabla \otimes \vec{v})^\intercal). \end{cases} \tag{2}$$

Here the unknowns are: the particle velocity $\vec{v} = \vec{v}(x, y, z, t)$ (the derivative of the local displacement vector with respect to time) and the symmetric stress tensor T, which has 6 independent components T_{xx}, T_{yy}, T_{zz}, T_{xz}, T_{yz}, T_{xz}. Force $\vec{F} = \vec{F}(x, y, z, t)$ denotes the right-hand side. Density ρ [kg/m^3] and two Lame parameters λ, μ [Pa] are the known possibly space-dependent medium parameters. In the equation (2) $\otimes$ stands for $\vec{a} \otimes \vec{b} = \mathbf{A}_{ij}$, $A_{ij} = a_i \cdot b_j$ and $\nabla \cdot \vec{v} = \operatorname{div} \vec{v}$.

Here we also use zero initial conditions. The following boundary condition is typically imposed: $T \cdot \vec{n} = \vec{f}(x, y, z, t)$, where $\vec{n}$ is a unit vector normal to the boundary ∂E.

Elastic equations (2) accurately describe body waves: longitudinal wave propagating with the speed $c_p = \sqrt{\frac{\lambda + 2\mu}{\rho}}$ and shear wave propagating with the speed $c_s = \sqrt{\frac{\mu}{\rho}}$, surface waves: Rayleigh wave, Love wave.

1.3. Dorovsky Model Equations

The following system of PDEs governs wave propagation in the Dorovsky model [4, 8, 11]:

$$
\begin{cases}
\vec{u}_t + \frac{1}{\rho_s}(\nabla \cdot \mathbf{h})^\intercal + \frac{1}{\rho_0}\nabla p = \vec{F}, \\
\vec{v}_t + \frac{1}{\rho_0}\nabla p = \vec{F}, \\
\mathbf{h}_t + \mu\left(\nabla \otimes \vec{u} + (\nabla \otimes \vec{u})^\intercal\right) + \left[\left(\lambda - \frac{\rho_s}{\rho_0}K\right)(\nabla \cdot \vec{u}) - \frac{\rho_f}{\rho_0}K(\nabla \cdot \vec{v})\right]\mathbf{I} = 0, \\
p_t - (K - \alpha\rho_0\rho_s)(\nabla \cdot \vec{u}) + \alpha\rho_0\rho_f(\nabla \cdot \vec{v}) = 0.
\end{cases}
\tag{3}
$$

In each infinitesimal medium volume there is a rigid skeleton and interconnected pores saturated with a fluid (typically water or oil for geophysical applications). The unknown functions in this system are: skeleton velocity (derivative of displacement with respect to time) $\vec{u} = \vec{u}(x, y, z, t)$, fluid velocity (derivative of displacement with respect to time) $\vec{v} = \vec{v}(x, y, z, t)$, minus stress tensor of the rigid skeleton $\mathbf{h} = \mathbf{h}(x, y, z, t)$, pore fluid pressure $p = p(x, y, z, t)$. Force $\vec{F}$ denotes the right-hand side.

The medium is described by the following parameters: $\rho_s = (1 - \beta)\rho_{s0}$, $\rho_f = \beta\rho_{f0}$, $\rho_0 = \rho_s + \rho_f$, where ρ_{s0}, ρ_{f0} are real physical densities of the rigid skeleton and the saturating fluid, respectively; β is the volumetric porosity of the medium defined by $\beta = \frac{V_{pores}}{V_{total}}$.

The remaining medium parameters K, μ, α are the elastic parameters of the saturated medium which are defined based on c_{p1}, c_{p2}, c_s (explained below) and already given ρ_0, ρ_s, ρ_f by the following relations:

$$
\mu = \rho_s c_s^2,
\tag{4}
$$

$$
K = \frac{\rho_0 \rho_s}{2\rho_f}\left(c_{p1}^2 + c_{p2}^2 - \frac{8}{3}\frac{\rho_f}{\rho_0}c_s^2 - \sqrt{(c_{p1}^2 - c_{p2}^2)^2 - \frac{64}{9}\frac{\rho_f \rho_s}{\rho_0^2}c_s^4}\right),
\tag{5}
$$

$$
\alpha_3 = \frac{1}{2\rho_0^2}\left(c_{p1}^2 + c_{p2}^2 - \frac{8}{3}\frac{\rho_s}{\rho_0}c_s^2 + \sqrt{(c_{p1}^2 - c_{p2}^2)^2 - \frac{64}{9}\frac{\rho_f \rho_s}{\rho_0^2}c_s^4}\right),
\tag{6}
$$

$$
\alpha = \rho_0\alpha_3 + K/\rho_0^3.
\tag{7}
$$

Known possibly space-dependent medium parameters c_{p1}, c_{p2}, c_s are the wave velocities of the first (fast) longitudinal wave, second (slow) longitudinal wave and shear wave, respectively. So, the Dorovsky model describes three kinds of body waves: two longitudinal ones and a shear wave. It also describes surface waves, like the linear elastic model.

We use zero initial conditions and the following boundary condition:

$$\begin{cases} p = P(x, y, z, t), & x, y, z \in \partial E, \ t > 0, \\ \mathbf{h} \cdot \vec{n} \cdot \vec{n} = H(x, y, z, t), & x, y, z \in \partial E, \ t > 0, \\ \mathbf{h} \cdot \vec{n} \cdot \vec{\tau} = 0, & x, y, z \in \partial E, \ t > 0. \end{cases} \tag{8}$$

Here $\vec{n}$ is a unit normal to the boundary, $\vec{\tau}$ is a unit vector tangential to the boundary (two linearly independent vectors in 3D case). Note that setting $P \equiv 0$, $H \equiv 0$ results in the free surface boundary condition in the case of open pores.

2. Numerical Method

Systems of PDEs (1), (2), and (3) are first-order systems that can be easily written in the matrix form

$$\vec{q}_t + A_x \vec{q}_x + A_y \vec{q}_y + A_z \vec{q}_z = \vec{f}, \tag{9}$$

where vector $\vec{q} = \vec{q}(x, y, z, t)$ contains all unknown functions, while known matrices A_x, A_y, A_z are defined by the combination of the appropriate material parameters. Initial conditions $\vec{q}^{(0)} = \vec{0}$. Boundary conditions can be generally written as a linear relation [6, 8]

$$B \cdot \vec{q}(x, y, z, t) = \vec{b}(x, y, z, t), \quad x, y, z \in \partial E, \ t > 0, \tag{10}$$

and will be discussed in more detail in subsection 2.3.

Below we describe construction of the numerical scheme for the above equations using the grid-characteristic method (GCM).

2.1. Operator Splitting

First of all, we want to simplify this three-dimensional system ($x, y, z \in \mathbb{R}^3$) by consecutive solutions of one-dimensional problems. This can be achieved by a coordinate splitting procedure. For an operator splitting scheme with s stages we need to perform the following procedure (see [9] for details in the 2D case):

```
for i in 1,...,s:
    perform stepX(α_i^x · dt)
    perform stepY(α_i^y · dt)
    perform stepZ(α_i^z · dt)
```

Here, *perform stepX* means find $\vec{q}^{(n+1)}$ for $\vec{q}$ satisfying the system $\vec{q}_t + A_x \vec{q}_x = \vec{0}$ and $t^{(n+1)} - t^{(n)} = \alpha_i^x \cdot dt$. For stepY and stepZ the similar formulae are applied with the appropriate matrix (A_y or A_z) and spatial derivative ($\frac{\partial}{\partial y}$ or $\frac{\partial}{\partial z}$) with the values from the previously done step as the starting $\vec{q}^{(n)}$.

Thus, an operator splitting scheme is defined by the coefficients α_i^j, $1 \leq i \leq s$, $j \in \{x, y, z\}$. Several examples are given in Tables 1–3. Although the last scheme theoretically demonstrates the highest approximation order, we chose the first scheme for our simulations in this work due to its high efficiency (one stage, $s = 1$) and relatively good performance. Also note that if a high-order scheme is used, one might need smaller dt since $\tau = \alpha_i^j dt$ should satisfy the stability condition, and some $|\alpha_i^j| > 1$. For instance, with the Y7-4 scheme one needs to make 13/3 times more one-dimensional steps for each 3D time step, and the dt value must be decreased approximately $\max_{i,j} |\alpha_i^j| \approx 1.7$ times, increasing the total number of time steps accordingly.

Therefore, a simulation with the high-order Y7-4 scheme takes 7.4 times longer than the one with the XYZ scheme on the same mesh.

The application of the right-hand side can be viewed as another operator in the splitting procedure. However, since in the problems considered right-hand side is usually a point source limited in time, we apply it only once per time step after the homogeneous equations have been solved by the operator splitting technique with respect to spatial coordinates.

Table 1. Coefficients of the XYZ splitting scheme: $s = 1$, 1st order of approximation

i	α_i^X	α_i^Y	α_i^Z
1	1	1	1

Table 2. Coefficients of the 3D Strang splitting scheme [2]: $s = 3$, 2nd order of approximation

i	α_i^X	α_i^Y	α_i^Z
1	0	0	1/2
2	0	1/2	0
3	1	1/2	1/2

Table 3. Coefficients of the Y7-4 splitting scheme [2]: $s = 7$, 4th order of approximation, $\phi_1 = \frac{1}{2 - \sqrt[3]{2}}$, $\phi_2 = -\frac{\sqrt[3]{2}}{2 - \sqrt[3]{2}}$

i	α_i^X	α_i^Y	α_i^Z
1	0	0	$\phi_1/2$
2	0	$\phi_1/2$	0
3	ϕ_1	$\phi_1/2$	$(\phi_1 + \phi_2)/2$
4	0	$\phi_2/2$	0
5	ϕ_2	$\phi_2/2$	$(\phi_1 + \phi_2)/2$
6	0	$\phi_1/2$	0
7	ϕ_1	$\phi_1/2$	$\phi_1/2$

2.2. One-Dimensional Case

Consider a one-dimensional system of equations, resulting from the operator splitting procedure defined above:

$$\vec{q}_t + A_x \vec{q}_x = \vec{0}. \tag{11}$$

Since original systems of PDEs (1), (2), and (3) are hyperbolic, matrix A_x has a full set of eigenvectors. It is correct for A_y and A_z too. We combine all eigenvectors as columns of a matrix and denote that matrix as Ω^{-1} – an inverse to a matrix Ω; we can do that since Ω^{-1} has full rank. Then, if we put all eigenvalues corresponding to eigenvectors in Ω^{-1} into the diagonal of a diagonal matrix Λ, the following relation will be valid: $A_x = \Omega^{-1}\Lambda\Omega$. Let us multiply (11) by the matrix Ω on the left:

$$\Omega \cdot \vec{q}_t + \Omega \cdot \Omega^{-1}\Lambda\Omega \cdot \vec{q}_x = \vec{0}, \tag{12}$$

$$(\Omega\vec{q})_t + \Lambda\Omega\vec{q}_x = \vec{0}. \tag{13}$$

Assuming matrix Ω to be constant and not depending on x, we obtain

$$(\Omega\vec{q})_t + \Lambda\,(\Omega\vec{q})_x = \vec{0}. \tag{14}$$

Introduce new unknown vector – the so called Riemann invariants $\vec{\omega} = \Omega\vec{q}$, we obtain a system of independents transport equations with respect to each component of $\vec{\omega}$:

$$\vec{\omega}_t + \Lambda\vec{\omega}_x = \vec{0}. \tag{15}$$

For each scalar equation $w_t + aw_x = 0$, where $w = \omega_i$, $a = \lambda_i$, the characteristic property is fulfilled: $w(x_m, t^{(n+1)}) = w(x_m - a\tau, t^{(n)})$, where $\tau = t^{(n+1)} - t^{(n)}$. Value $w_* = w(x_m - a\tau, t^n)$ can be obtained by using some interpolation procedure. Usually, a polynomial interpolation is used; in this work we used a third-order interpolation polynomial built on a four-point stencil in the internal points, resulting in a third-order scheme. This scheme closely resembles the known Rusanov scheme. Note that for positive and for negative λ_i the stencil points used for interpolation are different, which is important to preserve the stability properties of the scheme. Treatment of points near the boundary is discussed in the next subsection.

Finally, when we have computed each $\omega_i^{(n+1)}$ with the appropriate λ_i, we can return to the original unknowns using the formula $\vec{q}^{(n+1)} = \Omega^{-1}\vec{\omega}^{(n+1)}$.

The stability condition is the standard Courant condition $c \cdot dt/h < 1$, where $c = \max_i |\lambda_i|$.

For an efficient implementation we have precomputed matrices Ω and Ω^{-1} analytically. Of course, they depend upon medium properties – parameters of the corresponding PDE. During the simulation at each time step matrix-vector multiplication $\Omega\vec{q}$ and $\Omega^{-1}\vec{\omega}$ is performed quickly and the sparse nature of Ω and Ω^{-1} is taken into account. For larger matrices like the ones resulting from the Dorovsky model (3) utilizing symbolic algebra software like *Wolfram Mathematica* [12] or *Python*'s SymPy library proves to be beneficial.

2.3. Boundary Conditions

The scheme presented above cannot be implemented directly near the boundary because several points in the stencil required for interpolation are located outside the computational domain. In the framework of the grid-characteristic method we extend the computational grid by two ghost points on each side, allowing us to perform the same computations everywhere. Then, in order for the simulation to be accurate, i.e. for the setting of the appropriate boundary conditions, we utilize the following scheme:

1. fill ghost points with values from the closest point on the boundary in order to minimize reflections;
2. perform a special correction to set correct values on the boundary.

The first item approximates zero incoming values from outgoing characteristics – the ones that are outside the computational domain. The second item performs a correction based on the formula [5, 6, 8]:

$$\vec{q}^{(n+1)} = \vec{q}^{in} + \Omega^{out}(B \cdot \Omega^{out})^{-1} \cdot (\vec{b} - B\vec{q}^{in}), \tag{16}$$

where B and $\vec{b}$ are defined in (10), $\vec{q}^{in}$ is $\vec{q}$ after step 1 (with values updated only from those characteristics which stay inside the domain), Ω^{out} is a rectangular matrix, columns of which correspond to the outgoing characteristics. $\Omega^{out}(B \cdot \Omega^{out})^{-1}$ are precomputed analytically.

2.4. Contact Conditions

In many cases the wave propagates through several media with significantly varying properties. Using the most general and accurate mathematical model can be prohibitive for large simulations: for example, for the Dorovsky model (3) we have to store 13 floating-point values per point, which is 3.25 more than for the acoustic model (1), and there are also more operations involved. Also, some numerical discretizations of complex PDEs do not allow setting some of the parameters to zeros to treat special cases. Running one simulation on multiple grids, possibly with different equations on each one, is a popular approach to deal with such issues. In this subsection we present the technique to organize explicit contact between two grids.

Consider two grids representing two media, denoted by lower indices a and b (in this subsection this does not mean differentiation). We cover the computational domain in such a way that the points in grid a which are located exactly on the interface coincide with the points in grid b, which are also located exactly on the interface. Thus, for those physical points we will have two grid nodes: $\vec{q_a}$ in grid a, and $\vec{q_b}$ in grid b. Note that $\vec{q_a}$ and $\vec{q_b}$ can have different sizes and different components from different governing PDEs. In the general form we write the contact condition as

$$C \begin{bmatrix} \vec{q_a} \\ \vec{q_b} \end{bmatrix} = \vec{c}, \qquad (17)$$

where C is a rectangular matrix $R \times (n_a + n_b)$, n^a – number of components of $\vec{q_a}$, n_b – number of components of $\vec{q_b}$, R – total number of outgoing characteristics for both grids.

The boundary correction (16) can be written in the following form:

$$\vec{u}_i^{(n+1)} = \Phi_i \vec{u}_i^{in} + \vec{f_i}, \quad i \in \{a, b\}. \qquad (18)$$

Matrices Φ_i are known, vectors $\vec{f_i}$ are unknown. Substituting (18) into (17), we obtain a system of linear algebraic equations with respect to all components of $\vec{f_i}$, $i \in \{a, b\}$. The system has a unique solution if the boundary corrector matrices B_i were chosen correctly (for outgoing characteristics).

Thus, we get the following algorithm [5, 6, 8]:
1. run one step of the simulation on both grids for the internal points (and for boundary points using ghost cells), obtain $\vec{q}_i^{in}$ for $i \in \{a, b\}$;
2. solve the small algebraic system (17) with respect to $[\vec{f_a} \ \vec{f_b}]^\mathsf{T}$;
3. perform correction according to formula (16) for both grids, computing $\vec{q}_i^{(n+1)}$, $i \in \{a, b\}$.

For the contact between an acoustic medium governed by equations (1) and a fluid-saturated medium governed by the Dorovsky equations (3) the following contact conditions should be implemented [7]:

$$\begin{cases} (-||\mathbf{h}|| \cdot \vec{n}, \vec{n}) = -P_a, \\ (-||\mathbf{h}|| \cdot \vec{n}, \vec{\tau}) = 0, \\ (1 - \beta)(\vec{u}, \vec{n}) + \beta(\vec{v}, \vec{n}) = (\vec{V_a}, \vec{n}), \\ \frac{\rho_f}{\beta \rho_0} \cdot p = P_a. \end{cases} \qquad (19)$$

Here P_a and $\vec{V_a}$ denote pressure and velocity in the acoustic medium, respectively.

2.5. Parallel Algorithms

This subsection discusses the implemented parallel algorithms for using modern high-performance computing systems. For parallelization in a distributed memory system, MPI technology is used, in a shared memory system – OpenMP technology is used. The utilized grid-characteristic method on structured grids belongs to the class of explicit numerical methods. This allows using classical approaches to parallelization – the principle of geometric parallelism. The computational domain (grid) is divided into parts (blocks) with overlaps, the width of the overlaps is determined by the spatial scheme stencil. At each time step, data is exchanged in the border nodes (in overlapping parts). OpenMP technology (*pragma omp for*) is used to accelerate the basic scheme node loop. Thus, the computational algorithm successfully works at systems with distributed memory, with shared memory and in hybrid systems.

3. Simulation Results

3.1. Homogeneous Space

Our first simulation models wave propagation from a point-source vertical force applied at the centre of cubic computational domain with time dependence in the form of the Ricker impulse with the peak frequency of 30 Hz. The model size was 800 m × 800 m × 800 m. It was covered by a computational grid with step size of 2 m. Time step was 0.8 ms to satisfy the Courant stability condition, 200 time steps were taken. In one simulation, we use the linear elastic model with the parameters $c_p = 2000$ m/s, $c_s = 1300$ m/s, $\rho = 1450$ kg/m^3. In the second case, we used the Dorovsky model with similar parameters: $c_{p1} = 2000$ m/s, $c_{p2} = 450$ m/s, $c_s = 1300$ m/s, $\rho_0 = 1450$ kg/m^3, $\rho_f = 100$ kg/m^3, $\beta = 10\%$. Result of the simulation is presented in the Fig. 1.

(a) Simulation with the elastic model, absolute velocity $|\vec{v}|$

(b) Simulation with the porous Dorovsky model, absolute skeleton velocity $|\vec{u}|$
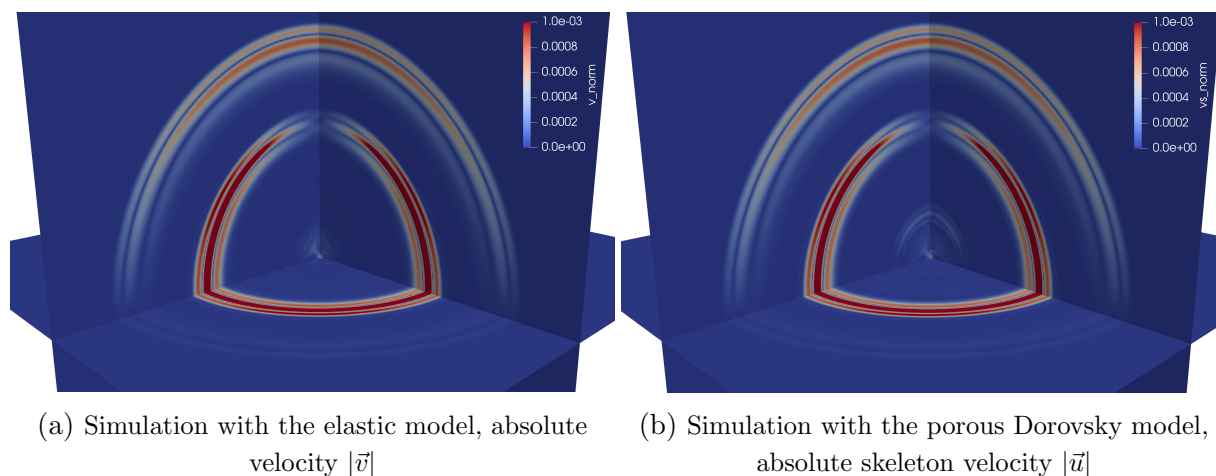
Figure 1. Slices of the absolute velocity. Pressure wave and shear waves are clearly seen in both simulations. The second pressure wave propagates with the low speed $c_{p2} < c_s$ only in the Dorovsky model

3.2. Bottom Sediments

We simulated wave propagation from a point source in a combination of a water layer, described by the acoustic equations (1), and a deformable water-saturated layer of bottom sediments, modelled by the Dorovsky equations (3). The three-dimensional case was considered. We used well-known water parameters: density $\rho = 1000$ kg/m^3 and wave velocity $c = 1500$ m/s. We used the following parameters for the Dorovsky model: porosity $\beta = 10\%$, physical water density $\rho_{f0} = 1000$ kg/m^3, physical skeleton density $\rho_{s0} = 1500$ kg/m^3, $\mu = 2.2815e9$ Pa, $K = 2.642306867e9$ Pa, $\alpha = 2507.905873$ $m^5/(kg \cdot s^2)$, corresponding to wave velocities $c_{p1} = 2000$ m/s, $c_{p2} = 450$ m/s, $c_s = 1300$ m/s. The point source was set at the depth of 4 m with the Ricker impulse with the peak frequency of 30 Hz as the time dependence.

The computational domain with the size 700 m $\times$ 700 m $\times$ 300 m was covered with two cubic grids with the step of 2 m: one for the water layer (250 m), one for the bottom sediments (50 m). To satisfy the Courant stability condition the time step was set to 0.9 ms. Totally, 250 time steps were taken.

The simulation was carried out on a PC with an Intel(R) Core(TM) i7-10700 CPU 2.9 GHz and 15 GiB RAM. For better utilization of multiple cores on a shared memory system, we used 1 MPI process with 8 OpenMP threads. This 3D simulation took approximately 1.5 minutes.

In Fig. 2 one can see the simulated region consisting of two computational grids in contact with each other. Pressure values are shown in both grids. Longitudinal wave in the water layer and two longitudinal waves in the sediments are clearly seen. The shear wave in the sediments is not visible on the displayed image of pore pressure, but it can be seen in the plot of absolute velocities.
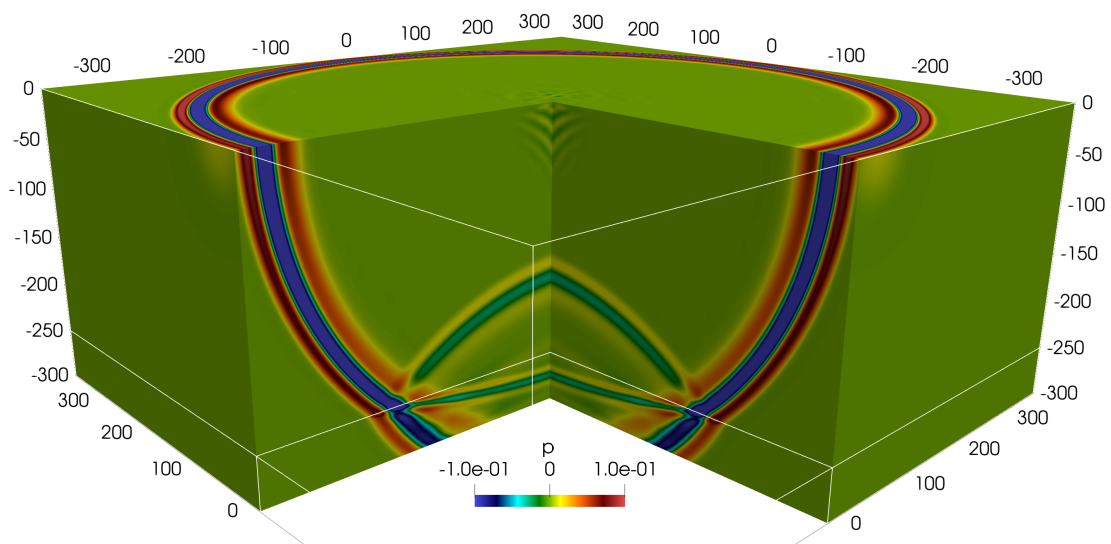
Figure 2. Spatial distribution of the pressure p in the model

Conclusion

The grid-characteristic numerical scheme on rectangular grids for the seismic wave simulation in a porous fluid-saturated medium governed by the Dorovsky model in the 3D case was

constructed. The analytical derivation of matrices Ω and Ω^{-1} makes an efficient implementation possible. The explicit contact conditions between an acoustic medium and a Dorovsky medium have been derived and implemented. We have simulated a problem in a realistic setting of a marine seismic survey process. The usage of the modern MPI and OpenMP technologies is the key for the real-scale computer simulation. Future works involves implementing contact between elastic and porous media and generalization to curvilinear grids in 3D, similar to the work [8] in the 2D case.

Acknowledgements

References

1. Aki, K., Richards, P.: Quantitative Seismology, Theory and Methods. University Science Books, second edn. (2002)

2. Auzinger, W., Koch, O., Thalhammer, M.: Defect-based local error estimators for high-order splitting methods involving three linear operators. Numerical Algorithms 70, 61–91 (2015). `https://doi.org/10.1007/s11075-014-9935-8`

3. Biot, M.: General theory of three dimensional consolidation. J. Appl. Phy. 12, 155–169 (1941). `https://doi.org/10.1007/s11075-014-9935-8`

4. Blokhin, A., Dorovsky, V.: Mathematical modelling in the theory of multivelocity continuum. Nova Science Publishers (1995)

5. Chelnokov, F.: Numerical modelling of deformational dynamic processes in media with complex structure. Ph.D. thesis, Moscow Institute of Physics and Technology, Moscow, Russia (2005)

6. Favorskaya, A., Zhdanov, M.S., Khokhlov, N.I., Petrov, I.B.: Modelling the wave phenomena in acoustic and elastic media with sharp variations of physical properties using the grid-characteristic method. Geophysical Prospecting 66(8), 1485–1502 (2018). `https://doi.org/10.1111/1365-2478.12639`

7. Golubev, V., Shevchenko, A., Petrov, I.: Taking into account fluid saturation of bottom sediments in marine seismic survey. In: Doklady Mathematics. vol. 100, pp. 488–490. Springer (2019). `https://doi.org/10.1134/S1064562419050107`

8. Golubev, V., Shevchenko, A., Petrov, I.: Simulation of seismic wave propagation in a multicomponent oil deposit model. International Journal of Applied Mechanics 12(08), 2050084 (2020). `https://doi.org/10.1142/S1758825120500842`

9. Golubev, V., Shevchenko, A., Petrov, I.: Raising convergence order of grid-characteristic schemes for 2D linear elasticity problems using operator splitting. Computer Research and Modeling 14(4), 899–910 (2022). `https://doi.org/10.20537/2076-7633-2022-14-4-899-910`

10. LeVeque, R.: Finite Volume Methods for Hyperbolic Problems. Cambridge Texts in Applied Mathematics, Cambridge University Press (2002). `https://doi.org/10.1017/CBO9780511791253`

11. Sorokin, K., Imomnazarov, K.: Numerical solving of the liner two-dimensional dynamic problem in liquid-filled porous media. Journal of Siberian Federal University. Mathematics & Physics 3(2), 256–261 (2010). `https://doi.org/10.1016/j.jcp.2012.11.001`

12. Wolfram Research, I.: Mathematica, Version 14.1, `https://www.wolfram.com/mathematica`, Champaign, IL, 2024